# Comparison of Faxén's correction for a microsphere translating or rotating near a surface

J. Leach,[1] H. Mushfique,[2,*] S. Keen,[1] R. Di Leonardo,[3] G. Ruocco,[3] J. M. Cooper,[2] and M. J. Padgett[1]
[1]*Department of Physics and Astronomy, University of Glasgow, Glasgow, Scotland*
[2]*Department of Electrical Engineering, University of Glasgow, Glasgow, Scotland*
[3]*INFM-CRS SOFT c/o Universitá di Roma "La Sapienza," I-00185 Roma, Italy*
(Received 28 August 2008; published 2 February 2009)

Boundary walls in microfluidic devices have a strong influence on the fluid flow and drag forces on moving objects. The Stokes drag force acting on a sphere translating in the fluid is increased by the presence of a neighboring wall by a factor given by Faxén's correction. A similar increase in the rotational drag is expected when spinning close to a wall. We use optical tweezers to confirm the translational drag correction and report the hitherto unmeasured rotational equivalent. We find that the corrections for the rotational motion is only required for particle-wall separations an order of magnitude shorter than that for the translational cases. These results are particularly significant in the use of optical tweezers for measuring viscosity on a picolitre scale.

DOI: 10.1103/PhysRevE.79.026301 PACS number(s): 47.15.−x, 66.20.−d

## INTRODUCTION

A knowledge of the drag forces acting on micron sized bodies moving within fluid is crucial in understanding the behavior of both microfluidic and biological systems [1,2]. On micron length scales, within liquid media, the Reynolds number is small, meaning that the forces arising from the viscosity of the fluid are dominant over its inertia. Viscosity is therefore the dominant force in all processes relying on transport, mixing or diffusion and hence measurement of the viscosity is paramount in understanding such systems. The viscosity $\eta$ of an incompressible fluid is defined as the coefficient relating the stress tensor $\boldsymbol{\sigma}$ to the velocity gradients,

$$\boldsymbol{\sigma} = \eta(\nabla \boldsymbol{v} + \nabla \boldsymbol{v}^T). \tag{1}$$

In the low Reynolds number limit, particles are inertialess and a constant force $\mathbf{F}$ or torque $\mathbf{T}$ is required to maintain them in a steady translational or rotational motion. The linear form of Stokes equation ensures that such forces and torques are proportional to the linear and angular velocities $\mathbf{U}$ and $\boldsymbol{\Omega}$ through the translational and rotational drag coefficients $\gamma$ and $\beta$,

$$\mathbf{F} = \gamma \mathbf{U}, \tag{2}$$

$$\mathbf{T} = \beta \boldsymbol{\Omega}. \tag{3}$$

Far from a boundary, the drag coefficients take the values $\gamma = 6\pi\eta a$ and $\beta = 8\pi\eta a^3$. Knowledge of particle size then allows one to extract viscosity from drag coefficients measurements. However, within a typical microfluidic or biological system these simple formulas no longer apply but the presence of confining walls results in an increased drag. Blind application of previous formulas would provide an overestimated viscosity $\eta^*$.

*j.leach@physics.gla.ac.uk

In this paper we observe the drag on a sphere moving near a wall. We confirm and extend previous measurements of translational drag [3–5], and report experimental determinations of rotational drag enhancement when approaching a wall.

## MICROSCOPIC RHEOLOGY

The motion of microscopic particles held by optical tweezers within fluid systems is used to measure hydrodynamic interactions, viscoelastic properties, and fluid flow [6–8]. Not least has been the measurement of local viscosity where either the thermally driven translation motion [9,10] or optically driven rotational speed of the particle [11–13] has been related to the drag coefficients. Each approach has its merits, but both drag coefficients are perturbed by the proximity of a surface. For the translational case, one method to determine the drag coefficient is monitoring the dynamics of an optically trapped particle [14]. The thermal motion of a trapped particle gives a root mean square displacement from the trap center of $\langle x^2 \rangle = k_B T/\kappa$, where $k_B$ is Boltzmann's constant, $\kappa$ is the spring constant of the optical trap, and $T$ is the temperature. The system is overdamped and hence the power spectrum of position fluctuations is Lorenzian with a cutoff frequency given by $f_0 = \kappa/2\pi\gamma$ and hence the translational drag coefficient is simply given by

$$\gamma = \frac{k_B T}{2\pi f_0 \langle x^2 \rangle}, \tag{4}$$

which is independent of the trap strength. As spontaneous rotational fluctuations are not easily detected, the rotational drag coefficient is measured by applying a known torque and monitoring the resulting rotation rate [12,15]. A circularly polarized trapping beam carries a spin angular momentum of $\hbar$ per photon and exerts a torque on a birefringent particle setting it into rotation. Calculation of the rotational drag coefficient is given by

 

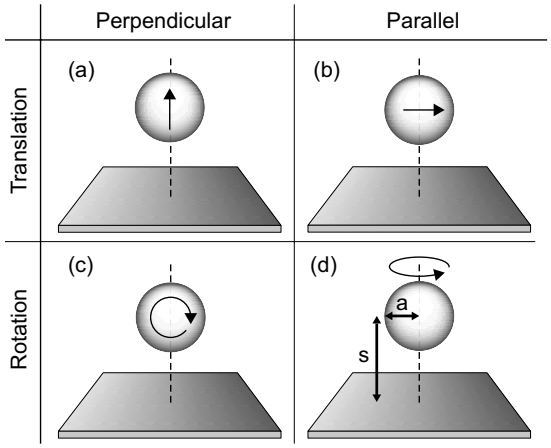


FIG. 1. Schematic representation of translation perpendicular (a) and parallel (b) to a surface and rotation of a sphere about an axis perpendicular (c) and parallel (d) to a surface normal. The radius of the sphere is given by $a$ and the distance between its center and the surface given by $s$.

$$\beta = \frac{P\Delta\sigma}{\hbar\omega\Omega}, \tag{5}$$

where $P$ is the power of the trapping beam of frequency $\omega$ and $\Delta\sigma$ is the change in the polarization state of the transmitted light ($\sigma = \pm 1$ for right and left hand circularly polarized light, respectively). Relating either Eq. (4) or Eq. (5) to viscosity requires knowledge of the particle radius, the uncertainty of which, coupled to the uncertainty of the power in the optical trap (in the rotational case), results in accuracies of around 10%. Surface corrections to the translational and rotation drag coefficients are therefore essential if the techniques are to be applied within microfluidic or confined biological systems.

## FAXÉN'S CORRECTIONS

One approach to solving Stokes' equation in the presence of boundaries is the method of reflections proposed by Smoluchowsky [16]. The method was employed by Faxén [17,18] to study particle-wall interactions and further developed by Happel and Brenner [19]. The linearity in Stokes' equations and boundary conditions means the solution can be expressed as a series of partial solutions. In the particle-wall case, the zeroth order corresponds to the flow produced by the particle in an unbounded fluid. The next correction is the reflection from the wall, that is, the solution of the Stokes equation having a boundary condition on the wall such that it cancels out the zero-order flow. The next term is the reflection of this last field from the particle boundary, and so on. Simple configurations, such as a single particle near a planar wall, can also be treated analytically in a bipolar coordinates system [20–23]. However, a "large" distance expansion is often more useful to estimate corrections. The method of reflections provides such expansions which can be quite accurate up to very short distances. The method was used by Faxén to correct the Stokes drag on a sphere translating near a wall; see Figs. 1(a) and 1(b). Faxén's corrections are expressed as a power series in the ratio of particle radius $a$ to the distance from the surface $s$. The corrections come in two forms dependent upon whether the particle motion is parallel or perpendicular to the surface. For a particle at a distance $s$ from a surface, the power series expansions to order $(a/s)^3$ of the translational drag in a direction both parallel and perpendicular to the surface are given by [24]

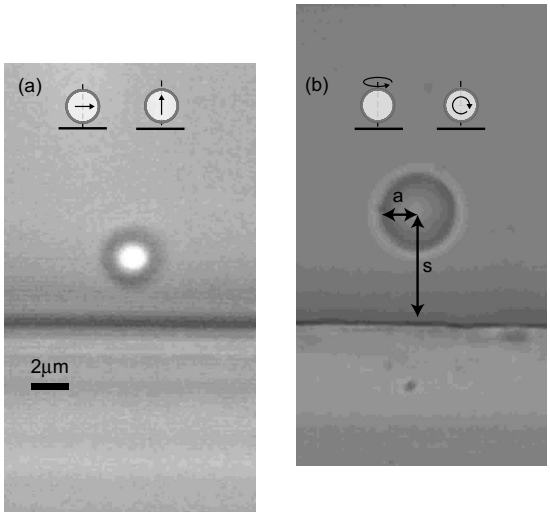


FIG. 2. Images of (a) the silica particle trapped close to the PDMS wall, where the translational drag coefficient is deduced by monitoring its residual Brownian motion, and (b) the spinning vaterite particle, where the change in rotational drag coefficient is deduced from its speed of rotation whilst driven by a constant optical torque.

$$\gamma^{\parallel} = \frac{\gamma}{1 - (9/16)(a/s) + (1/8)(a/s)^3}, \tag{6}$$

$$\gamma^{\perp} = \frac{\gamma}{1 - (9/8)(a/s) + (1/2)(a/s)^3}. \tag{7}$$

Similarly, the drag torque on a rotating sphere in the presence of a surface is also increased; see Figs. 1(c) and 1(d). This problem was considered initially in 1915 by Jeffery [23] who analyzed the torque acting on a sphere rotating about an axis parallel to a surface normal. Some years later, Dean and O'Neill [22,25] found the analytical solution to the situation where the axis of rotation of the sphere is perpendicular to the surface normal. A much simpler and more usable form is obtained by the method of reflections [19]. The sixth order term in Eq. (9) was derived by ourselves from the second wall reflection:

$$\beta^{\parallel} = \frac{\beta}{1 - (1/8)(a/s)^3}, \tag{8}$$

$$\beta^{\perp} = \frac{\beta}{1 - (5/16)(a/s)^3 + (15/256)(a/s)^6}. \tag{9}$$

It is helpful to note that within the adopted naming convention, a parallel or perpendicular geometry always corre-

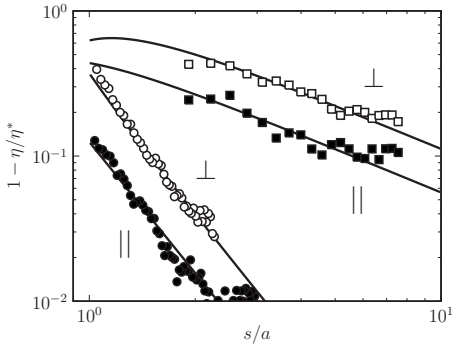


FIG. 3. Experimentally measured drag coefficients as a function of the separation of the sphere from the surface. Results for translation, perpendicular (□) and parallel (■) to a surface, and rotation about an axis perpendicular (○) and parallel (●) to the surface normal. The solid lines are the power series expansions of Faxén's correction given by Eqs. (6)–(9).

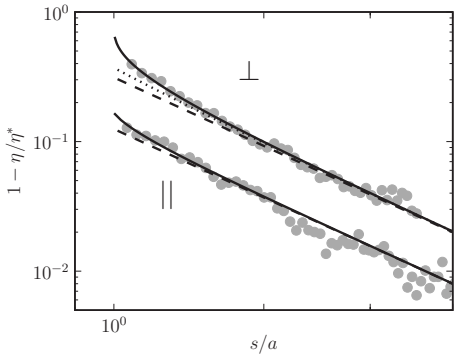


FIG. 4. Comparison between solutions to Faxén's correction for the rotation cases. The solid lines are the exact solutions [22,23], the dotted lines are the power series expansions in previous literature [25]. The dotted line is Eq. (9) which is the power series expansion that includes our sixth order final term. The experimental data points are plotted for comparison.

sponds to fluid flowing mostly parallel or perpendicular to the wall surface.

Of the four corrections shown in Fig. 1, only (a) and (b) [Eqs. (6) and (7)] have been experimentally verified [3–5] using optical tweezers [26] to trap a particle at known distances from the surface. In this work we also use optical tweezers, but to experimentally measure all four corrections, i.e., translation both perpendicular and parallel to the wall and rotation about an axis either parallel or perpendicular to the surface normal.

## EXPERIMENT

The microfluidic channels within which the probe particles were trapped were made using typical soft lithographic techniques, namely pattern transfer, deep dry etch, and replica moulding of the elastomeric polymer, poly(dimethylsiloxane), PDMS, Sylgard 184. The PDMS channels approximately 50 $\mu$m deep were fabricated and sealed with a cover slip (150 $\mu$m thick). The microfluidic channel was mounted as the sample cell on a computer controlled translation stage with a postioning repeatability of 40 nm. Both forms of the translation drag and the perpendicular rotational drag were made with the particles trapped at various distances from a channel wall, 10 $\mu$m above the sample cell floor (see Fig. 2). The rotational drag for spinning about an axis parallel to the surface normal was performed away from any walls as a function of height above the sample cell floor.

The rotational drag coefficients were measured using an optical tweezers based on a continuous-wave $\lambda=1064$ nm laser (Laser Quantum, Ventus 1064). Immediately prior to the objective lens (1.3NA, 100x Zeissplan-neofluar), the linearly polarized beam was passed through a quarter-wave plate aligned to convert the light's polarization to create a circularly polarized trap. The probe particles were vaterite crystals, grown according the recipe in Ref. [12] to a diameter of approximately 3 $\mu$m, with a birefringence of 0.1. These particles were trapped and brought closer to surfaces by using the $x,y$ (Prior) or $z$ (PiezoJena) translation stages. After passing through the sample cell, the transmitted laser light was collected through the condenser and a photodiode was used to observe intensity fluctuations resulting from the rotation of the trapped object. Rotation rates of the trapped particles were determined by analyzing the frequency spectrum of the intensity variations of the transmitted light [27].

For the measurement of translational drag the trapping laser was a $\lambda=800$ nm Ti:sapphire laser (SolsTiS, M Squared) and the probe particles were 2 $\mu$m diameter silica particles (Bangs Labs). The drag coefficient was determined from high-speed video images from which the center of mass motion of the trapped particle could be determined [28] and then fitted to a Lorentzian power spectrum giving the mean square displacement, the cutoff frequency, and hence the translational drag coefficient.

## RESULTS AND DISCUSSION

Figure 3 shows the experimentally measured correction to both the translational and rotational drag coefficients for micron sized particles as a function of distance from the surface. Any calibration issue depending upon particle size and laser power could be eliminated by using the same particle for all different distances and normalizing data to the bulk values obtained with the same particle trapped at many tens of radii from the wall. One possible concern is that the proximity of the ultrahigh NA trapping beam to the channel wall may have degraded the quality of the optical trap or the imaging of the particle motion and hence perturbed our measurements of the viscosity. In all our experiments we monitored the mean square displacement of the particle from the trap center. This did not change with distance from the wall leading us to believe that neither trap nor image degradation was an issue. For the data analysis of these cases, $s$ was calculated from the distance moved by the translation stages combined with a small distance offset left as a free parameter in the fitting. This allowed us to account for inaccuracies in measuring using the optical image and errors arising from the surface roughness of the PDMS channel. This was compared to the optical image to check for constancy and found to agree with the distance calculated from the optical image

to within 10%. As it was difficult to estimate the radius of the particles from the optical image to a high accuracy, the particle diameters were left as a free parameter in the fitting and compared afterward to the estimation from the optical image. Again, we found an agreement between the fit and the optical image to within 10%.

For the translational cases, we see excellent agreement between our measurements and the three term power series of Faxén's correction, Eqs. (6) and (7). One can see immediately that the rotational correction is required at much shorter separations than for the translational correction. The extremely short range nature of this interaction has previously been noted in relation to microrheology using spinning particles [11]. This differing length scale can be explained by considering the fluid flow fields created by translating and rotating spheres. For the translational case, the zero-order (no wall) flow field decays with $1/R$, where $R$ is the distance from the sphere. The ambient field around the particle is then corrected by a linear component of order $1/R$ producing a reduction in the speed of the particle. In contrast, for the rotational case the fluid flow decays faster, as $1/R^2$. The flow fields reflected from the wall are of the same order and the angular velocity of the spinning particle will be reduced by a fluid vorticity which scales with the gradient of the reflected ambient field and hence of order $1/R^3$. As a consequence, the influence of surfaces on translational or rotational particle dynamics occurs at different length scales. The extremely short range nature $[(s/a)-1 \ll 1]$ of the rotational case means that the power series needs to fit for a larger range of $s/a$, and consequently deviates more noticeably from the exact solution. Figure 4 compares the exact solutions (solid lines) [22,23] to different power series expansions (dashed and dotted lines) and experimental data (points). Although the power series expressed by Eqs. (8) and (9) do deviate from the exact solution, this discrepancy is not significant, except for when the distance between the surface and the particle is much less than one radius.

## CONCLUSIONS

We have experimentally verified the drag coefficients associated with the translation and rotation of a sphere, parallel and perpendicular to a surface. The hydrodynamical coupling between the surface and sphere is dramatically different for translation and rotation. For example, for the translation of a sphere parallel to the surface, a 10% increase in drag coefficient occurs at a distance of five radii, the same size of correction occurs for rotational motion only within one radii of the surface. These corrections are essential for accurate microrheology.

## ACKNOWLEDGMENT

The authors would like to thank Professor Rubinsztein-Dunlop for helpful discussions on the subject.

[1] L. D. Landau and E. M. Lifshitz, *Fluid Mechanics* (Pergamon, London, England, 1959).
[2] R. Larson, *The Structure and Rheology of Complex Fluids* (Oxford University Press, New York, 1999).
[3] A. Pralle, E. Florin, E. Stelzer, and J. Hörber, Appl. Phys. A: Mater. Sci. Process. **66**, S71 (1998).
[4] K. Vermeulen, G. Wuite, G. Stienen, and C. Schmidt, Appl. Opt. **45**, 1812 (2006).
[5] E. Schäffer, S. F. Nørrelykke, and J. Howard, Langmuir **23**, 3654 (2007).
[6] J.-C. Meiners and S. R. Quake, Phys. Rev. Lett. **82**, 2211 (1999).
[7] E. R. Dufresne, T. M. Squires, M. P. Brenner, and D. G. Grier, Phys. Rev. Lett. **85**, 3317 (2000).
[8] R. Di Leonardo, S. Keen, J. Leach, C. D. Saunter, G. D. Love, G. Ruocco, and M. J. Padgett, Phys. Rev. E **76**, 061402 (2007).
[9] G. Pesce, A. Sasso, and S. Fusco, Rev. Sci. Instrum. **76**, 115105 (2005).
[10] R. Brau, J. Ferrer, H. Lee, C. Castro, and B. Tam, J. Opt. A, Pure Appl. Opt. **9**, S103 (2007).
[11] A. I. Bishop, T. A. Nieminen, N. R. Heckenberg, and H. Rubinsztein-Dunlop, Phys. Rev. Lett. **92**, 198104 (2004).
[12] G. Knoner, S. Parkin, N. R. Heckenberg, and H. Rubinsztein-Dunlop, Phys. Rev. E **72**, 031507 (2005).
[13] S. J. Parkin, G. Knoner, T. A. Nieminen, N. R. Heckenberg, and H. Rubinsztein-Dunlop, Phys. Rev. E **76**, 041507 (2007).
[14] K. Berg-Sorensen and H. Flyvbjerg, Rev. Sci. Instrum. **75**, 594 (2004).
[15] M. E. J. Friese, T. A. Nieminen, N. R. Heckenberg, and H. Rubinsztein-Dunlop, Nature (London) **394**, 348 (1998).
[16] M. Smoluchowski, Bull. Int. Acad. Pol. Sci. Lett., Cl. Sci. Math. Nat., Ser. A **1**, 28 (1911).
[17] H. Faxén, Ann. Phys. **4**, 89 (1922).
[18] H. Faxén, Ark. Mat., Astron. Fys. **18**, 1 (1924).
[19] J. Happel and H. Brenner, *Low Reynolds Number Hydrodynamics* (Kluwer Academic Publishers, Dordrecht, 1983).
[20] M. Chaoui and F. Feuillebois, Q. J. Mech. Appl. Math. **56**, 381 (2003).
[21] M. O'Neill, Mathematika **10**, 13 (1963).
[22] W. R. Dean and M. E. O'Neill, Mathematika **10**, 13 (1963).
[23] G. B. Jeffery, Proc. London Math. Soc. **14**, 327 (1915).
[24] S. Kim and S. Karrila, *Microhydrodynamics* (Dover Publications, New York, 2005).
[25] M. D. A. Cooley and M. E. O'Neill, J. Inst. Math. Appl. **4**, 163 (1968).
[26] A. Ashkin, J. M. Dziedzic, J. E. Bjorkholm, and S. Chu, Opt. Lett. **11**, 288 (1986).
[27] T. A. Nieminen, N. R. Heckenberg, and H. Rubinsztein-Dunlop, J. Mod. Opt. **48**, 405 (2001).
[28] S. Keen, J. Leach, G. Gibson, and M. J. Padgett, J. Opt. A, Pure Appl. Opt. **9**, S264 (2007).